Plant Archives Vol. 20, Supplement 2, 2020 pp. 1082-1088 **e-ISSN:2581-6063 (online), ISSN:0972-5210**

CHARACTERIZATION AND CLINICAL APPLICATIONS OF SILVER NANOPARTICLES SYNTHESIZED FROM *CASSIA OBTUSIFOLIA* LEAVES EXTRACT

Laheeb Subhy Flaih and Narjis Hadi Al-Saadi*
Department of Chemistry, College of Science, University of Kerbala, Karbala, Iraq.
*Corresponding author E mail: narjis.h@uokebala.edu.iq

Abstract

Metal nanoparticles developed by nanotechnology have gained worldwide attention due to their extensive applications in biomedical and physiochemical fields. The aims of this study is green synthesis of silver nanoparticles from *Cassia obtusifolia* leaf extract as a reducing agent. The characterization of the synthesized silver nanoparticles and evaluated their clinical application were done. UV.-Vis. spectroscopy and the change in the color confirmed the formation of silver nanoparticles, which revealed a single peak at 410 nm. The possible functional groups of AgNPs solutions were identified by Fourier-transform infrared spectroscopy FTIR. Atomic force microscopy analysis revealed the average particle size of AgNPs reached to 57.42 nm. AgNPs were further, characterized by the characteristic peaks, which observed in the X-ray diffraction image. The results of clinical applications showed that the synthesized AgNPs prolonged the coagulation time by increasing prothrombin time and activated partial thromboplastin time as well as reduced platelet aggregation.
Keywords: Metals nanoparticles, Plant extracts, Clinical Application.

Introduction

Recently, silver nanoparticles (AgNPs) have received massive attention from the researchers. AgNPs play an important role in biology and medicine because of their appealing physiochemical properties among nanomaterial. This has been reported to have anti-fungal, anti-inflammatory, anti-viral, anti-angiogenic and anti-platelet activity (Benakashani *et al.*, 2016). By reaching nanoparticles size in a sure range (1-100 nm), their physical, chemical, and electrical properties will modulation (Khodashenas and Ghorbani, 2015). Nowadays, the fabrication of NPs concentrates on green synthesis from the different plant parts extract. The multifunctional agents used to reduce and stabilize plant extraction for biological synthesis on NPs use to carry out green chemistry (Beyene *et al.*, 2017). Plants or their extracts, which serve as reducing and capping agents for the synthesis of nanoparticle, are more beneficial than other biological methods, due to the exclusion of the elaborated process of culturing and preserving the cell, and can raise the synthesized nanoparticles for large-scale (Ibrahim, 2015). Plant crude extract contains novel secondary metabolites like alkaloids, phenolic acid, flavonoid and terpenoids which are fundamentally accountable for the reduction of ions into bulk metallic nanoparticle formation (Kuppusamy *et al.*, 2016).

Cassia obtusifolia L. belongs to the Leguminosae family (subfamily Caesalpinoideae) and is widely used as traditional herbal medicine (Jang and Yang, 2018). Types of *Cassia* have biological and therapeutic function such as immunomodulation, antioxidant, antimicrobial and hypo-lipidemia (Moteriya *et al.*, 2017). Antioxidants are very important to shield the cell and biological macromolecules from the degenerative reactions that free radical and reactive oxygen species are produced. Polyphenolic substances like (flavonoids and tannins) obtained from different plants and herbal extract are involved in the antioxidant activity of these extracts (Sudha *et al.*, 2017).

The present study aims to evaluate the use of *Cassia obtusifolia* leaves extract as a reduction agent for the synthesis of silver nanoparticles, and to investigate their clinical use.

Materials and Methods

Plant collection and chemicals

Fresh leaves of *Cassia obtuifolia* were collected from the garden of the University of Kerbala, College of Science. The leaves were cleaned using distilled water then deionized water and then crushed into small slice and stored for further used.

The chemicals, used in this research, were got from Hi Media Laboratories (India), Reagent World Inc. (USA), Merk, (USA), and Gainland Chemical Company (GCC), (UK). C.K. Prest 2 kit and Neoplastine CI Plus 5 kit (Stago) (China) were purchased form medical laboratories.

Preparation of aqueous leaf extract

Twenty grams of cut leaves were added into 200 mL of deionized water and boiled for 5, 10, and 15 minutes respectively, then filtered through filter paper Whatman No.1. The cassia leaves extract filtrate was used for the Ag NPs synthesis.

Synthesis of silver nanoparticles

For the synthesis of silver nanoparticles (AgNPs), the aqueous solution of (1mM) of $AgNO_3$ was prepared, and then various volumes of aqueous leaf extract were added into 50 mL of $AgNO_3$ solution for the reduction of Ag^+ ions. The mixture was incubated at 45 ºC and dark place. Ultracentrifugation at 8000 xg for 10 min was used to obtain purified silver nanoparticles and then the pellets were dried and stored at 4 ºC for further use.

Characterization of synthesized silver nanoparticles

UV-Vis spectroscopy : The synthesis of AgNPs was confirmed by the color exchange and UV-Vis absorption spectra. The absorbance of the solution mixture was measured at the period time and the maxima absorption was scanning by UV-Vis spectroscopy at range 300-700 nm.

Fourier-transform infrared spectroscopy (FTIR) : FTIR was used to recognize the functional groups of the cassia leaves extract of the biomolecules associated with AgNPs formation. The infrared spectra of the sample were measured with the KBr disk in the wavelength range of 400-4000 cm^{-1} using Shimadzu (8400S)/Japan FTIR spectrophotometer.

Qualitative phytochemical analysis : Gas chromatography and mass spectroscopy GC-Mass (Agilant) was used to analyze the chemical constituents of *Cassia obtuifolia* leaves extract. The analysis was done at University of Kashan, Iran. The instrument used electron ionization with two columns, Helium, Nitrogen, and zero air was used as carrier gas; the oven temperature was 400 °C, after getting chromatogram of GC-Mass for organic compounds, they were identified by comparing their spectra to those stored on the computer library.

X-ray diffraction (XRD) : The structure of synthesized AgNPs was performed using XRD analysis. Scherrer equation was used to calculate the crystal size of the synthesizing AgNPs. $D = 0.94\ \lambda/\beta\ COS\ \theta$, where D is the average crystallite domain size perpendicular to the reflecting planes, λ is the wavelength of x-ray, β is the full width at half maximum. A coated film of Ag NPs was formed on a glass plate and XRD pattern was investigated using Philips Xpert / Holland XRD Co-kα1 radiation (k=1.50456) in the range of 10° to 80°.

Atomic Force Microscopy (AFM) : The size and the surface properties of biosynthesized nanoparticles were visualized by atomic force microscopy (CSPM Scanning Probe Microscope) under normal atmospheric conditions. The samples were diluted with distilled water and then dropped onto glass slides, followed by air drying during 24h at room temperature. Highest measurement was obtained using AFM image analysis software at the University of Baghdad, Department of Chemistry.

Clinical application

(a) Measurement of coagulation factors PT and APTT

Collection of blood specimens : Twenty-three healthy blood volunteers (n=23) were enrolled for PT and PTT test. A 2.7 mL of the peripheral blood sample was collected in 3.2% sodium citrate tubes. The age of the blood donors ranging from 18 to 40 years old with no any medication such as anticoagulants, antiplatelet, antibiotics drugs as well as herbal drugs, vitamin or mineral supplement within 14 days before blood donation.

Preparation of Samples : The blood samples were centrifuged at 3000 xg for 15 minutes. The obtained plasma was treated with different concentrations of *Cassia obtusifolia* aqueous extract or AgNPs (25, 50 and 100µg/mL) with a ratio of 1:1 (plasma: extract), (plasma: Ag NPs) and incubated for 5 minutes at 37 °C.

Coagulation factors : Coagulation analyzer (Diagnostica Stago, France) was used to measure baseline coagulation screening tests PT and APTT. PT was measured using Neoplaastine CI plus 5 kit, whereas, C.K.PREST2 kit and 0.025 M calcium chloride were used to measurement APTT (Neofotistos *et al.*, 1998).

Prothrombin Time (PT) test : A metallic ball bearing was added into each cuvette, then the reconstituted human plasma (50 µL) was added and then incubated at 37 °C for 1 minute in the rotating rack. Clotting was initiated by adding (100 µL) of reconstituted recombiplastin. The time until clot formation was recorded automatically. The procedure was repeated with the sample that was prepared in (2.5.1.2).

Activated Partial Thromboplastin Time (APTT) test : A metallic ball bearing was added into each cuvette, then the reconstituted CK PREST 2 (50 µL) and human plasma (50 µL) were added and incubated for 3 minutes at 37 °C in the rotating rack. Clotting was initiated with the addition of $CaCl_2$ (50 µL) and the time was recorded automatically. The procedure was repeated with the sample that was prepared in (2.5.1.2).

(b) Platelet aggregation

Samples preparation : Platelet- rich plasma (PRP) and platelet- poor plasma (PPP) were treated with blood from five healthy donors that had at least two weeks free from any medication. Blood specimens were collected by venipuncture in test tubes containing buffered sodium citrate. Blood tubes were centrifuged for 10 min at 800-900 xg and 1 ml of platelet- rich plasma (PRP) was gained from the supernatant fraction. Repeat centrifugation for 20 min at 4000 xg to obtain (PPP). After preparation, PRP was used immediately.

Light transmission aggregometry : The impact of AgNPs on spontaneous or induced platelet aggregation was tested using the Thombo-Aggregometer/ France. The mixture of reaction for spontaneous aggregation tests consists of 275 µL of PRP induced with 30 µL of adenosine diphosphate (ADP). Data was recorded at 405 nm with the chronology two channel recorders connected to a computer. The same procedure was repeated with the addition 15 µL of different concentrations of Ag NPs (25, 50 and 100 µg/mL) respectively. (Laloy *et al.*, 2014).

(c) Hemolysis assay

The blood hemolysis method which is an *in vitro* disruption of human red blood cells (RBCs) by plant extract was carried out as described by the method (Bouma, 2002) so, the blood specimen of healthy nonsmoker donor was used in this test:

Generally, 30 µL of AgNPs solution was added to 0.2 mL of blood at the concentrations (25, 50 and 100 µg/mL) respectively and mixed well for 5 seconds. To avoid unnecessary hemolysis, a 20 mL of normal saline was added. The mixture was centrifuged for 10 minutes at 3000 xg. After this, the mixture's optical density (O.D.) was measured at 540 nm. In addition, determine the percentage of hemolysis done by AgNPs to 100% hemolysis is the principle of this test. So, diluting blood with 100 fold of distilled water was performed for complete hemolysis (100%). Triton X-100 used as a positive control, after measuring the absorption, the hemolysis percentage was calculated as the following equation:

$$\%\ \text{Hemolysis} = (AT-AS)\ /(A\ 100\%-AS) \times 100\%$$

Where, AT is the absorbance of the test solution, AS is absorbance of the normal saline, and A 100% is the absorbance of 100% hemolysis.

Statistical analysis

The results of this study were statistically analyzed using an independent t-test and One-Way Analysis of

Variance (ANOVA), p-Value ≤ 0.05 was considered significant.

Results

Synthesis of silver nanoparticles

The addition of silver nitrate to the aqueous leaf cassia extract resulted in a color change from greenish to brown and this the first evidence for the Ag NPs synthesis in compared with silver nitrate solution as blank (figure 1).

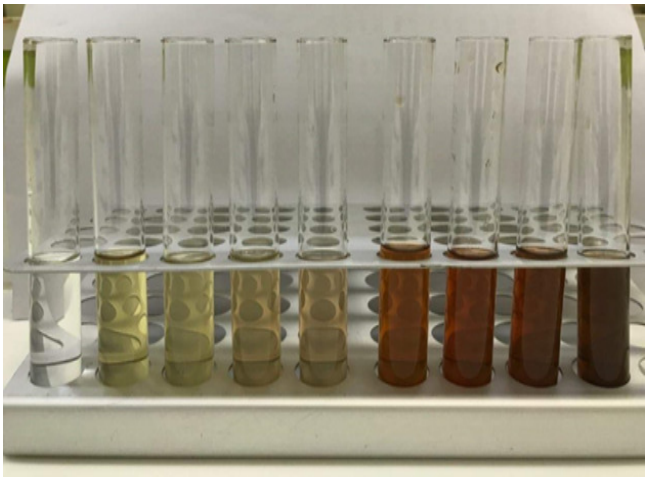

Fig. 1 : The gradually change in color of the synthesized Ag NPs

Characterization of the synthesized silver nanoparticles

UV-Vis spectroscopy : The synthesis Ag NPs were firstly characterized with their absorbance spectra in UV-Vis spectroscopy at room temperature, clear and broad peak observed at around 410 nm, which are signification for synthesis AgNPs (Figure 2).

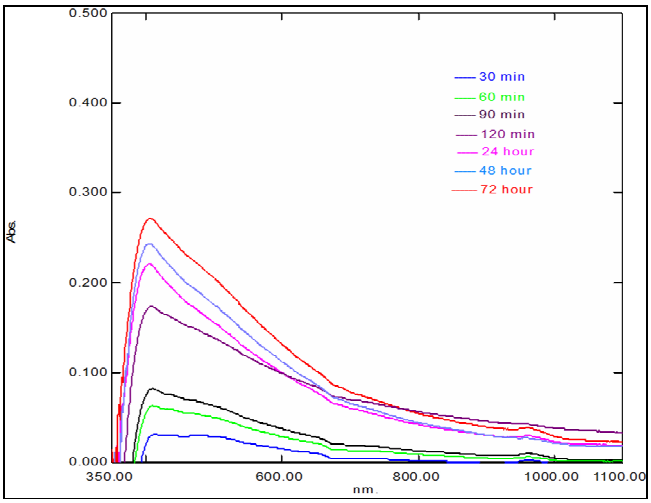

Fig. 2 : UV-Visible spectra of synthesized Ag NPS by 4 ml extract boiling for 10 min over time.

GC-MS Analysis : Gas chromatography and mass spectroscopy analysis of cassia leaves extract were carried out. The chromatogram shows 6 peaks of the most constituents (Figure 3). The most constituents included, (E) -9- Octadecenoic acid, Oleic acid, 9-Octadecenamide, Estra-1,3,5 (10)-trien-17, beta-ol and 1-(+)-Ascorbic acid 2,6-dihexad.

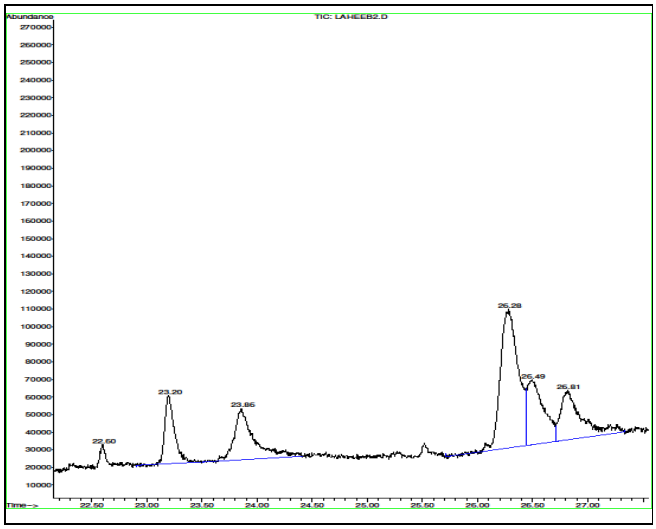

Fig. 3 : GC-mass of Cassia leaf extract

Fourier transform infrared spectroscopy (FTIR) : FTIR measurement was done to distinguish between biomolecules of aqueous leaf *cassia obtusifolia* extract that responsible for capping and effective stabilization of synthesized AgNPs. The results showed noticeable bands of absorbance at peaks 3379.40, 2933.83, 1614.47, 1510.31, 1417.73, 1072.46, 858.236 cm^{-1} (figure 4A). In addition, the FTIR of AgNPs synthesized by cassia extract at 3288.74, 2920.32, 1647.26, 1516.10, 1462.09, 1220.98, 1060.88, 671.25 and 858.236 cm^{-1} respectively (Figure 4B). The absorption shifted at 3379.40 cm^{-1} to 3288.74 cm^{-1} matches to the stretching vibration of the hydroxyl group, a peak at 2933.83 cm^{-1} shifted to 2920.32 cm^{-1} matches to the stretching vibration of C-H alkanes. Peaks at 1614.47, 1510.31 and 1417.73 cm^{-1} respectively shifted to 1647.26, 1516.10, 1462.09 cm^{-1} respectively, Corresponds to C=O, C=C and N-H of primary and secondary amines and amide. Peaks at 1072.46, 858.236 and 669.32 cm^{-1} shifted to 1060.88, 858.236 and 671.25 cm^{-1} respectively, matches to C-O bond of ethers. The peaks at 538.16 and 504.44 cm^{-1} signified the possibility of an alkyl halide in cassia leaf extract (figure 4).

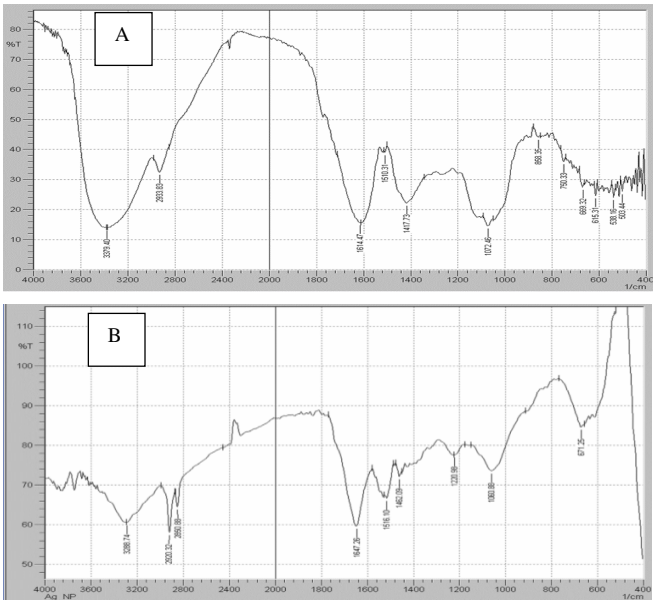

Fig. 4 : FTIR spectrum of (A) Cassia leaf extract (B) synthesized Ag NPs

X-ray diffraction (XRD) : The results of XRD suggested the crystallization of the bioorganic phase takes place on the surface of the AgNPs or vice versa. Mostly the boarding of peaks in the XRD patterns of solids is referred to crystal size effects. XRD analysis for the synthesized AgNPs showed three distinct diffraction peaks of 27.8597", 32.2135", and 46.3619^0 at 2θ values (Figure 5). The average size of crystals for the synthesized AgNPs was estimated to be 23.24 nm. Also showed the crystallographic planes for each angle value in comparing with the standard 2θ of silver nanoparticles according to Standard X-ray Diffraction Powder Patterns.

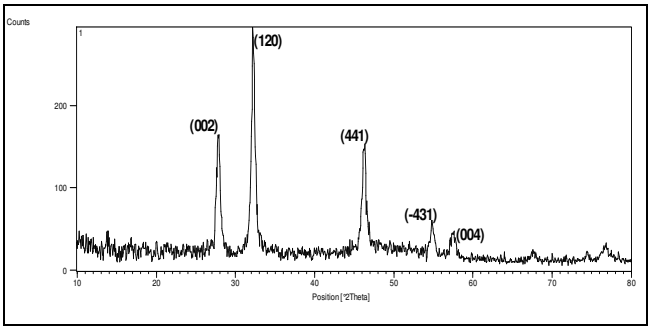

Fig. 5 : X-ray diffraction of synthesized Ag NPs from Cassia aqueous leaf extract.

Atomic Force Microscopy (AFM) : The topography of the surface and the size of particles were determined by atomic force microscopy. The figure (6-a) showed two- dimensional image of AgNPs showing in clusters of spherical shapes for Ag NPs synthesis by 4 ml of leaf extract boiling for 10 min. The figure (6-b) showed three- dimensional image of AgNPs, which, revealed a population of homogeneous particles, and the average size of particles was 57.42 nm.

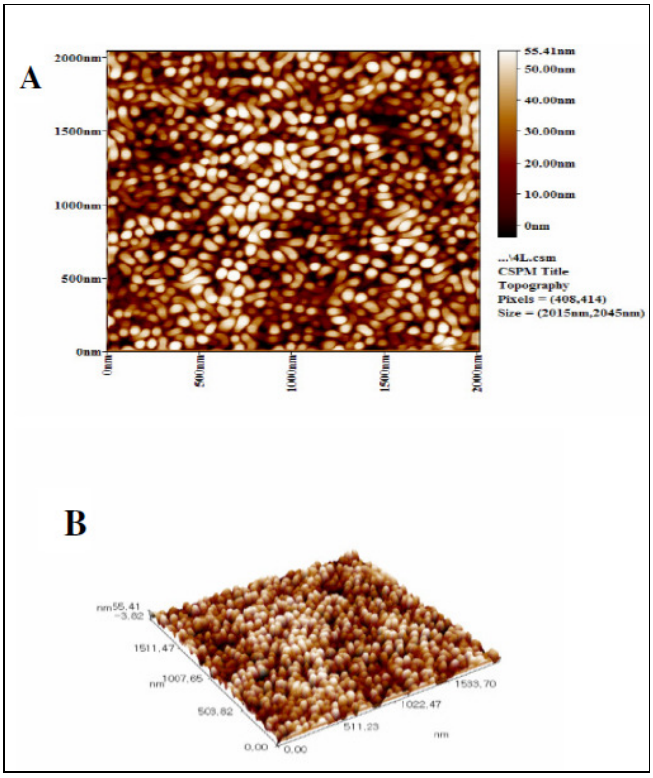

Fig. 6 : AFM analysis of silver nanoparticles synthesized by 4 ml of aqueous leaf extract of Cassia boiling for 10 min (A) Two-dimensional image (B) three- dimensional image

Coagulation factors

The coagulation tests were performed involving PT and APTT. The results were statistically analyzed as mean and standard deviation (SD). They appeared that synthesize AgNPs cause a highly significant increase ($p<0.001$) in PT at the concentrations (25, 50, 100 µg/mL) respectively compared with PT of control and there is a significant difference ($p<0.001$) between all groups. As well as, APTT has increased significantly ($p<0.001$) with an increased concentration of AgNPs (Table 1).

Table 1 : Prothrombin Time (PT) and (APPT) of blood samples with and without Ag NPs.

	Groups N=23	Mean ± SD	P- value	P-value
PT	Control	14.01 ± 1.3	< 0.001	< 0.001
	25 µg/ml Ag NPs	21.93 ± 2.57		
	Control	14.01 ± 1.3	< 0.001	
	50 µg/ml Ag NPs	22.12 ± 2.94		
	Control	14.01 ± 1.3	< 0.001	
	100 µg/ml Ag NPs	21.40 ± 2.8		
APTT	Control	31.64 ± 4.24	< 0.001	< 0.001
	25 µg/ml Ag NPs	47.36 ± 5.98		
	Control	31.64 ± 4.24	< 0.001	
	50 µg/ml Ag NPs	48.16 ± 7.16		
	Control	31.64 ± 4.24	< 0.001	
	100 µg/ml Ag NPs	48.17 ± 7.16		

P-value ≤ 0.05 is significant

Platelet aggregation

The results of the synthesizing AgNPs in the concentration (25, 50,100 µg/mL) respectively showed a decreased platelet aggregation compared with the control (figure 7).

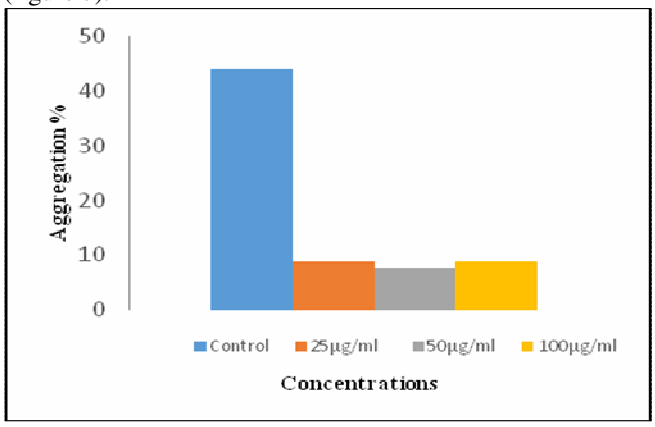

Fig. 7 : Platelet aggregation at different concentration of Ag NPs

Hemolytic activity

The hemolytic activity of the silver nanoparticles from Cassia was tested against normal human erythrocytes. Synthesized silver nanoparticles at a concentration (25 µg/mL) showed the reducing of hemolysis (4.4%) comparing with the concentrations of other (Figure 8).

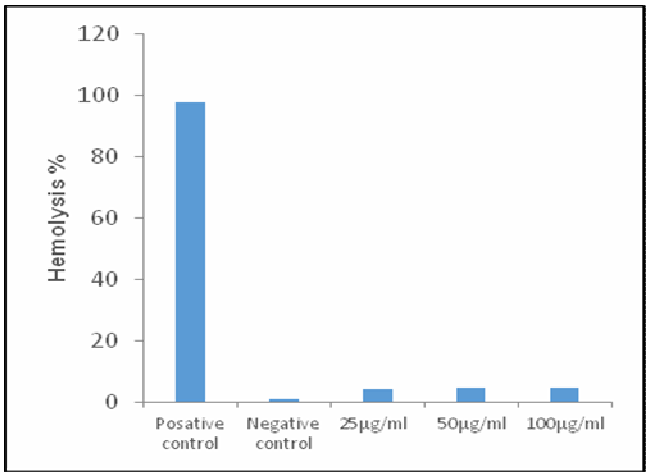

Fig. 8 : The percentage of Hemolysis induced by Ag NPs. Triton X-100 as a positive control and normal saline as a negative control.

Discussion

The color change from yellow to dark brown is the first evidence for the synthesis of silver nanoparticles which indicated the reduction of silver particles, the synthesis of silver nanoparticles are depending on the time exposure of reducing agents to metal ions so, when the incubation time of silver with the reducing agents increased, the synthesis of SNPs is increased (Rocchetti *et al.*, 2017). Ag NPs are known to display a maximum UV–Visible absorption of UV-Visible at the range of 400-500 nm due to surface plasmon resonance (Ashraf *et al.*, 2016). Silver nanoparticles were characterized at the different periods times of the reagent mixture using UV-Vis spectrum. Plant extract compassion in charge of reducing silver nitrate and stabilization of silver nanoparticles. GC mass analysis of aqueous leaf extract of *Cassia Obtusifolia* detected the chemicals compounds as ratio. The major compound was oleic acid which, is the mean fatty acid present in the extract, it has noticed to be accountable to prevent agglomeration of the nanoparticle (Andrade *et al.*, 2013), 9-Octadecenoic acid,(E)- has been shown to have biological activity, including antioxidant, anti-inflammatory and antibacterial effect (Kang *et al.*, 2018). The presence of hexadecanoic acid appears as a stabilizing agent and thus repression the aggregation of silver nanoparticles and to conserve the formed of silver nanoparticles(Socrates and Mohan, 2019). In addition, the FTIR analysis indicates that carboxyl (-C=O), hydroxyl (-OH) are a presence in both Cassia extract and synthesized AgNPs which was earlier confirmed its present in the compound that detected by GC-mass spectroscopy. The absorption shifted at 3379.40 cm^{-1} to 3288.74 cm^{-1} corresponds to the stretching vibration of the hydroxyl group, a peak at 2933.83 cm^{-1} shifted to 2920.32 cm^{-1} corresponds to the stretching vibration of C-H alkanes. Peaks at 1614.47, 1510.31 and 1417.73 cm^{-1} respectively shifted to 1647.26, 1516.10, 1462.09 cm^{-1} respectively, Corresponds to C=O, C=C and N-H of primary and secondary amines and amide. Peaks at 1072.46, 858.236 and 669.32 cm^{-1} shifted to 1060.88, 858.236 and 671.25 cm^{-1} respectively, corresponds to C-O bond of ethers the aromatic C-H (out of plane bend) and C-H bond of alkene. The shift in the IR bands suggesting the reaction of silver ions and synthesis of nanoparticles in the extract (Pavia *et al.*, 2008).

These groups act as reducing agents and stabilizers for silver nanoparticles and agglomeration prevent. The strong ability of the carbonyl group of the amino acids to binding with metals, suggests the formation of a layer coating silver nanoparticles and expressible as a stabilizing agent prevents agglomeration in the aqueous medium (Awwad *et al.*, 2013).

The results of X-ray diffraction showed that the synthesized silver nanoparticles are crystalline. The Brag reflection at 27.8597°, 32.2135°, and, 46.3619°, at 2θ values, confirmed the crystalize structure of silver nanoparticles. The values of these angles was comparing with the standard 2θ of silver nanoparticles according to Standard X-ray Diffraction Powder Patterns (Morris, 1979).

The intensity of peak reflects the high degree of crystallite of the silver nanoparticles. The diffraction peak was broad signalize that the crystallite size is very small (Sangeetha *et al.*, 2016). Previous studies showed the crystalline structure using XRD analysis of biosynthesized AgNPs. Another study showed the similar XRD results which confirmed the crystallinity of synthesizing AgNPs from *Ricinus communis* var. *carmencita* leaf extract (Ojha *et al.*, 2017).

In this study, the average particle size of synthesizing silver nanoparticles was 57.24 nm. Similar study obtained the average size 57 nm of synthesized silver nanoparticles from *Moringa oleifera* leaf extract (Prasad and Elumalai, 2011). Previous studies reports that synthesizing AgNPs from commercially available plant extracts, such as *Solanum tricobatum, Syzygium Cumini, Centella Asiatica,* and *Citrus Sinensis* have irregular shapes, and the particle size was found to be 53, 41, 52 and 42 nm respectively (Logeswari *et al.*, 2013).

In this study, the activity of AgNPs on the coagulation of blood was investigated based upon coagulation tests, PT and APTT. PT reflects the substantial coagulation pathway whereas APTT reflects the substantial coagulation pathway in haemostasis process. This study showed that both PT and APTT were significantly prolonged. Ag NPs activity could be attributed to the content of active component present in the cassia extract. It can be noticeable to point out that aqueous extract component is effective on PT and APTT such as oleic acid that presents as a main fatty acid in the aqueous extract of cassia which known for its protective against cardiovascular and neurodegenerative diseases (Debbabi *et al.*, 2017). Due to the presence of fibrinogen-thrombin fatty acid ternary complexes, and potentially fibrinogen fatty acid aggregates, the fibrin polymerization is delay and this explain the maximal prolonged clotting time by the fatty acids. (Tanka-Salamon *et al.*, 2016).

Silver nanoparticles blocked thrombin- induced platelet aggregation in a concentration dependent method. More than 80% of inhibition was evaluated at a concentration of 50 µg/mL of nanoparticles, so this significantly reduced the slope of aggregation per minute. The platelet aggregation induced other physiological agonists like ADP under the same condition. Control group which was treated similarly but without addition nanoparticles exhibited the normal aggregation. Aggregation was significantly minimized the platelet originally exposed to NPs, suggestive of continued interaction between nanoparticles and platelets (Shrivastava *et al.*, 2009).

The toxicity of metal nanoparticles was checked by hemolysis. Hemolysis happens when the red cells come in contact with water, so it is important to check the materials before use. it has been well known that the permissible limit of hemolysis for biomedical substances should be less than 5% in all states. (Autian, 1975). *In vitro* study, the cytotoxicity of silver nanoparticles is assayed against human blood erythrocytes (RBCs). In medicine, the vascular system may be taking silver nanoparticles via injection or oral administration, so frequently maybe direct interaction between silver nanoparticles and RBC occur. The earlier report on silver nanoparticles has demonstrated that small particles have higher hemolytic activity than large particles, in the contract that in silica nanoparticles increase hemolytic activity increased with large particles(Lin and Haynes, 2010)

Conclusion

The aqueous *Cassia Obtusifolia* leaf extract is a good source for synthesis AgNPs. UV-Vis spectra showed the maximum absorbance at 410 nm. XRD analysis promoted the crystalline nature of synthesized AgNPs. The average of particle size to be 57.24 nm was indicated by AFM analysis. The synthesized AgNPs exhibited a good anticoagulation activity by prolongation of the time of both PT and APTT, decreased platelet aggregation and have a few effects on blood hemolysis.

References

Andrade, P.; Silva, V.; Maciel, J.; Santillan, M.; Moreno, N.; Valladares, L.D.L.S.; Bustamante, A.; Pereira, S.; Silva, M. And Aguiar, J.A. (2013). Preparation And Characterization Of Cobalt Ferrite Nanoparticles Coated With Fucan And Oleic Acid. Lacame 2012. Springer.

Ashraf, J.M.; Ansari, M.A.; Khan, H.M.; Alzohairy, M.A. And Choi, I. (2016). Green Synthesis of Silver Nanoparticles And Characterization of Their Inhibitory Effects on Ages Formation Using Biophysical Techniques. Scientific Reports, 6: 20414.

Autian, J. (1975). Biological Model Systems For The Testing of The Toxicity of Biomaterials. Polymers In Medicine And Surgery. Springer.

Awwad, A.M.; Salem, N.M. and Abdeen, A.O. (2013). Green Synthesis of Silver Nanoparticles Using Carob Leaf Extract And Its Antibacterial Activity. International Journal of Industrial Chemistry, 4: 29.

Benakashani, F.; Allafchian, A.R. and Jalali, S.A.H. (2016). Biosynthesis of Silver Nanoparticles Using Capparis Spinosa L. Leaf Extract and Their Antibacterial Activity. Karbala International Journal of Modern Science, 2: 251-258.

Beyene, H.D.; Werkneh, A.A.; Bezabh, H.K. and Ambaye, T.G. (2017). Synthesis Paradigm and Applications of Silver Nanoparticles (Agnps), A Review. Sustainable Materials and Technologies, 13: 18-23.

Bouma, M. (2002). Pharmaceutical Development of The Novel Metal-Based Anticancer Agents Nami-A And Ap 5280.

Debbabi, M.; Zarrouk, A.; Bezine, M.; Meddeb, W.; Nury, T.; Badreddine, A.; Sghaier, R.; Bretillon, L.; Guyot, S. and Samadi, M. (2017). Comparison of The Effects of Major Fatty Acids Present In The Mediterranean Diet (Oleic Acid, Docosahexaenoic Acid) And In Hydrogenated Oils (Elaidic Acid) On 7-Ketocholesterol-Induced Oxiapoptophagy In Microglial Bv-2 Cells. Chemistry and Physics of Lipids, 207: 151-170.

Ibrahim, H.M. (2015). Green Synthesis and Characterization of Silver Nanoparticles Using Banana Peel Extract And Their Antimicrobial Activity Against Representative Microorganisms. Journal of Radiation Research and Applied Sciences, 8: 265-275.

Jang, S.H. and Yang, D.K. (2018). The Combination of *Cassia obtusifolia* L. and Foeniculum Vulgare M. Exhibits A Laxative Effect On Loperamide-Induced Constipation of Rats. Plos One, 13: E0195624.

Kang, M.-C.; Ham, Y.-M.; Heo, S.-J.; Yoon, S.-A.; Cho, S.-H.; Kwon, S.-H.; Jeong, M.S.; Jeon, Y.-J.; Sanjeewa, K. and Yoon, W.-J. (2018). Anti-Inflammation Effects of 8-Oxo-9-Octadecenoic Acid Isolated From Undaria Peterseniana In Lipopolysaccharide-Stimulated Macrophage Cells. Excli Journal, 17: 775.

Khodashenas, B. and Ghorbani, H.R. (2015). Synthesis of Silver Nanoparticles With Different Shapes. Arabian Journal of Chemistry.

Kuppusamy, P.; Yusoff, M.M.; Maniam, G.P. and Govindan, N. (2016). Biosynthesis of Metallic Nanoparticles Using Plant Derivatives and Their New Avenues In Pharmacological Applications–An Updated Report. Saudi Pharmaceutical Journal, 24: 473-484.

Laloy, J.; Minet, V.; Alpan, L.; Mullier, F.; Beken, S.; Toussaint, O.; Lucas, S. and Dogne, J.-M. (2014). Impact of Silver Nanoparticles on Haemolysis, Platelet Function And Coagulation. Nanobiomedicine, 1: 4.

Lin, Y.-S. and Haynes, C.L. (2010). Impacts of Mesoporous Silica Nanoparticle Size, Pore Ordering, and Pore Integrity on Hemolytic Activity. Journal of The American Chemical Society, 132: 4834-4842.

Logeswari, P.; Silambarasan, S. and Abraham, J. (2013). Ecofriendly Synthesis of Silver Nanoparticles From Commercially Available Plant Powders and Their Antibacterial Properties. Scientia Iranica, 20: 1049-1054.

Morris, M.C. (1979). Standard X-Ray Diffraction Powder Patterns: Section 16--Data For 86 Substances, Department of Commerce, National Bureau of Standards.

Moteriya, P.; Padalia, H. and Chanda, S. (2017). Characterization, Synergistic Antibacterial and Free Radical Scavenging Efficacy of Silver Nanoparticles Synthesized Using Cassia Roxburghii Leaf Extract. Journal of Genetic Engineering and Biotechnology, 15: 505-513.

Neofotistos, D.; Oropeza, M. and Ts′ Ao, C.-H. (1998). Stability of Plasma For Add-on Pt And Aptt Tests. American Journal of Clinical Pathology, 109: 758-763.

Ojha, S.; Sett, A. and Bora, U. (2017). Green Synthesis of Silver Nanoparticles By Ricinus Communis Var. Carmencita Leaf Extract and Its Antibacterial Study. Advances In Natural Sciences: Nanoscience And Nanotechnology, 8: 035009.

Pavia, D.L.; Lampman, G.M.; Kriz, G.S. and Vyvyan, J.A. (2008). Introduction to Spectroscopy, Cengage Learning.

Prasad, T. and Elumalai, E. (2011). Biofabrication of Ag Nanoparticles Using *Moringa oleifera* Leaf Extract And Their Antimicrobial Activity. Asian Pacific Journal of Tropical Biomedicine, 1: 439-442.

Rocchetti, G.; Lucini, L.; Chiodelli, G.; Giuberti, G.; Montesano, D.; Masoero, F. and Trevisan, M. (2017). Impact of Boiling on Free and Bound Phenolic Profile and Antioxidant Activity of Commercial Gluten-Free Pasta. Food Research International, 100: 69-77.

Sangeetha, R.; Niranjan, P. and Dhanalakshmi, N. (2016). Characterization of Silver Nanoparticles Synthesized Using The Extract of The Leaves of Tridax Procumbens. Res. J. Med. Plant, 10: 159-166.

Shrivastava, S.; Bera, T.; Singh, S.K.; Singh, G.; Ramachandrarao, P. and Dash, D. (2009). Characterization of Antiplatelet Properties of Silver Nanoparticles. Acs Nano, 3: 1357-1364.

Socrates, S.H. and Mohan, S.C. (2019). Phytochemical Analysis of Flower Extracts of Different Cassia Species By Using Gas Chromatography-Mass Spectrometry. Biological Chemistry, 13: 1-11.

Sudha, A.; Jeyakanthan, J. and Srinivasan, P. (2017). Green Synthesis of Silver Nanoparticles Using *Lippia nodiflora* Aerial Extract and Evaluation of Their Antioxidant, Antibacterial and Cytotoxic Effects. Resource-Efficient Technologies, 3: 506-515.

Tanka-Salamon, A.; Komorowicz, E.; Szabó, L.; Tenekedjiev, K. and Kolev, K. (2016). Free Fatty Acids Modulate Thrombin Mediated Fibrin Generation Resulting In Less Stable Clots. Plos One, 11: E0167806.